Neutron-diffraction study of liquid iodine

C. Andreani
Dipartimento di Fisica, Università di Roma "Tor Vergata," Via E. Carnevale, Roma, I-00173, Italy

M. C. Bellissent-Funel
Laboratoire Leon Brillouin, Centre d'Etudes Nucléaires de Saclay, 91191 Gif-sur-Yvette CEDEX, France

F. P. Ricci*
Dipartimento di Fisica, Università di Roma "La Sapienza," Piazza Aldo Moro 2, Roma, I-00185, Italy

M. A. Ricci
Dipartimento di Fisica, Università di L'Aquila, Via Vetoio, Coppito, L'Aquila, I-67010, Italy
(Received 17 April 1991)

Accurate neutron-diffraction measurements on saturated liquid iodine, up to $Q=16$ Å^{-1}, at $T=409$ K are presented. The intermolecular structure factor has been derived and a study performed on the presence of orientational correlations and their contribution to the intensity distribution. The experimental intermolecular pair correlation function has been compared with the results of a simulation performed using the anisotropic atom-atom pair potential proposed by Rodger, Stone, and Tildesley [Mol. Phys. **63**, 173 (1988)], giving excellent agreement. A comparison with previous neutron and x-ray data is also discussed.

PACS number(s): 61.20.−p, 61.12.Ex, 61.12.Gz

INTRODUCTION

The structure factors of liquid halogens show high modulations ascribable to the presence of strong orientational correlations among neighboring molecules. These arise from the anisotropy of both overlap and dispersive contributions to the intermolecular potential. Among liquid halogens, iodine shows the largest anisotropy and therefore is the most interesting system in order to investigate the orientational correlations in the liquid state.

Despite this interest, very few microscopic studies of the physical properties of liquid iodine have been published. As far as its static structure is concerned, only one neutron-diffraction study [1], up to only 6 Å^{-1}, and one x-ray diffraction study [2] are available in the literature. Moreover from the comparison of these data large discrepancies show up in the shape of the structure factor $S(Q)$ (e.g., the first peak intensities differ of $\sim 10\%$). Similar systematic variations between the neutron and x-ray data have also been found for liquid chlorine and bromine [3] and their origin is still a matter of controversy in that the intermolecular structure factor derived from x-ray data is doubtful.

Recently Rodger, Stone, and Tildesley [4,5] proposed an anisotropic atom-atom pair potential, namely, $A2$, to describe a variety of liquid phase properties of Cl_2, Br_2 and I_2. However the test of this potential on the structure of liquid iodine was not considered to be conclusive [5], being the Q range of the experimental data of Ref. [1] too short. As a matter of fact a limited Q range does not allow a reliable determination of the radial correlation function, which is the appropriate function to be compared with the simulation results.

Moreover the shortage of the Q range in the experimental data also prevented the determination of the intramolecular distance d from the neutron data [1]. The latter has been found to vary from 2.666 Å in the gas phase [6], through 2.715 Å in the crystalline phase [7], to 2.904 Å in the metallic phase [8,9] at 21 GPa: these findings suggest that d is strongly affected by the interations with neighboring molecules. As a consequence the determination of d in the liquid phase can be very instructive.

In this paper we report accurate neutron measurements of the $S(Q)$ function of liquid iodine up to $Q=16$ Å^{-1}. The wider Q range allows a proper comparison with the simulation studies in terms of the radial distribution function and a reliable assessment of the interatomic distance within the molecule.

EXPERIMENTAL APPARATUS AND MEASUREMENTS

Neutron-diffraction measurements were performed on the $7-C2$ spectrometer installed at the Orphee reactor (Centre d'Etudes Nucléaires de Saclay). The wavelength of the incident neutron beam was $\lambda=0.7045$ Å; further details about the spectrometer performances can be found in Ref. [10].

The temperature of the experiment was $T=409$ K and was controlled within ± 0.5 K by a cylindrical foil vanadium furnace driven by a thermoregulator [10]: the temperature gradient was controlled by two thermocouples sitting on the bottom and top of the sample container and was always less than 0.5 K. Both sample and furnace were placed under vacuum inside the standard 7-$C2$ bell jar.

Saturated liquid iodine was contained in a sealed cylindrical quartz tube of inner and outer diameters of 7.3 and 8.3 mm, respectively. The neutron beam was impinging on a 4-cm height of liquid.

The following runs have been performed on (1) sample plus container inside furnace I_{S+C}^{expt}; (2) empty container inside furnace I_C^{expt}; (3) furnace I_{VAC}^{expt}; (4) cadmium rod (diameter equal to the outer diameter of the cell) inside furnace I_{Cd}^{expt}; (5) vanadium rod (diameter equal to the sample diameter) inside furnace I_V^{expt}; (6) ^{3}He at $p=3.7$ atm inside sample container in furnace $I_{^3\text{He}}^{\text{expt}}$.

Runs (1), (2), and (6) have been performed at $T=409$ K, (4) and (5) at room temperature, while (3) at both temperatures. The ^{3}He pressure has been chosen in order to give the same transmission as the iodine sample. In Fig. 1 we report $I_{S+C}^{\text{expt}}, I_C^{\text{expt}}, I_{VAC}^{\text{expt}}$ and $I_{\text{Cd}}^{\text{expt}}$, normalized at 10^6 monitor counts, as a function of Q.

The intensities have been recorded by a position sensitive detector (PSD) [10], having 640 equally spaced cells in the 2θ range 0–126°. The average total counts collected at each cell are $2\times10^5, 1\times10^5, 8\times10^3$, and 4×10^3 for runs (1)–(4), respectively. This gives an average statistical uncertainty on the single scattering from the sample of the order of 0.3%.

DATA ANALYSIS

The differential scattering cross section $d\sigma/d\Omega$ for liquid iodine has been derived from the experimental intensities, following the procedure proposed in Ref. [11].

From the intensities $I_{S+C}^{\text{expt}}, I_C^{\text{expt}}, I_{^3\text{He}}^{\text{expt}}$ and I_V^{expt} the appropriate backgrounds have been subtracted

$$I_\alpha^B = I_{\text{Cd}}^{\text{expt}} + T_\alpha (I_{VAC}^{\text{expt}} - I_{\text{Cd}}^{\text{expt}}) , \tag{1}$$

where T_α is the transmission of scatterer α reported in Table I, together with other quantities of interest for the data analysis, for iodine, vanadium and quartz.

The single-scattering intensity from the sample I_S can be evaluated as

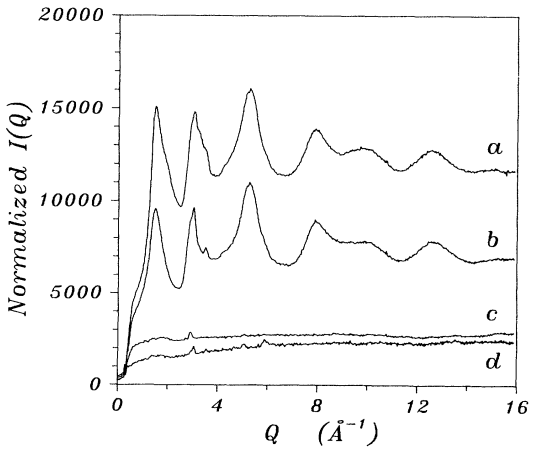

FIG. 1. Normalized scattered intensities as a function of Q. Curve a, I_{S+C}^{expt}; curve b, I_C^{expt}; curve c, I_{VAC}^{expt}; curve d, $I_{\text{Cd}}^{\text{expt}}$.

TABLE I. Values of the transmission T, coherent scattering length b, scattering cross section σ_{sc}, and absorption cross section at $\lambda=0.7$ Å, σ_a for I atom, SiO_2, and V, following Ref. [12].

	T	b (10^{-12} cm)	$\sigma_{\text{sc}}(b)$	$\sigma_a(b)$
I	0.925	0.528	4.52	2.72
SiO_2	0.984	1.58	10.65	0.07
V	0.756	−0.0382	4.95	2.00

$$I_S = I_{S+C}^{\text{expt}} - I_{S+C}^{\text{B}} - \gamma(I_C^{\text{expt}} - I_C^{\text{B}}) - \frac{m}{m+1} \times [I_{S+C}^{\text{expt}} - I_{S+C}^{\text{B}} - \gamma(I_C^{\text{expt}} - I_C^{\text{B}})]_{Q\to\infty} , \tag{2}$$

where γ and m account for sample absorption and multiple-scattering fraction, respectively. The latter values have been evaluated by using the routine described in Ref. [11] for a beam with a Gaussian profile [full width at half maximum (FWHM) 1 cm]. Both quantities are smooth Q functions and are well represented by

$$\gamma = 0.9414 - 2.816\times10^{-4}Q + 1.409\times10^{-4}Q^2 - 6.44\times10^{-6}Q^3 \tag{3}$$

and

$$m = 6.551\times10^{-2} + 6.4\times10^{-6}Q - 5.5\times10^{-7}Q^2 .$$

As far as γ is concerned we checked that these values agree with those derived from the ^{3}He run.

The differential scattering cross section $d\sigma/d\Omega$ for liquid iodine has been finally derived as

$$\frac{d\sigma}{d\Omega} = \left[\frac{d\sigma}{d\Omega}\right]_V \frac{I_S}{I_V}\frac{T_V}{T_S}\frac{\rho_V}{\rho_S} , \tag{4}$$

where I_V is the measured scattering intensity for vanadium corrected for background, multiple and inelastic scattering; ρ_V and ρ_S are the number densities of vanadium and iodine (7.2×10^{-2} and 1.86×10^{-2} atom/Å^3, respectively).

The differential scattering cross-section data for $Q\geq7$ Å^{-1} have been fitted to the isolated molecule scattering cross section according to

$$B\left[1+\frac{\sigma_c}{\sigma_{\text{sc}}}\exp\left[-\frac{l^2Q^2}{2}\right]\frac{\sin(Qd)}{Qd}\right] , \tag{5}$$

where l^2 is the mean-square amplitude of the thermal vibration and $\sigma_c=4\pi b^2$. The results of the fit are $l=(9\pm2)\times10^{-2}$ Å, $d=(2.70\pm0.02)$ Å, and $B=(0.360\pm0.001)b/sr$; data and their fit are reported in Fig. 2. We observe that the intramolecular distance in the liquid phase coincides within the error with the value found in the crystalline phase [7]. We note an excellent agreement (of few parts per thousand) of B with the theoretical value for the iodine atom $\sigma_{\text{sc}}/4\pi$ (see Table I and Fig. 2). This means that the inelastic effects are very small. However these have been evaluated, assuming that the inelasticity contribution in the liquid is the same as in an assembly of noninteracting molecules [13]. With this hypothesis we

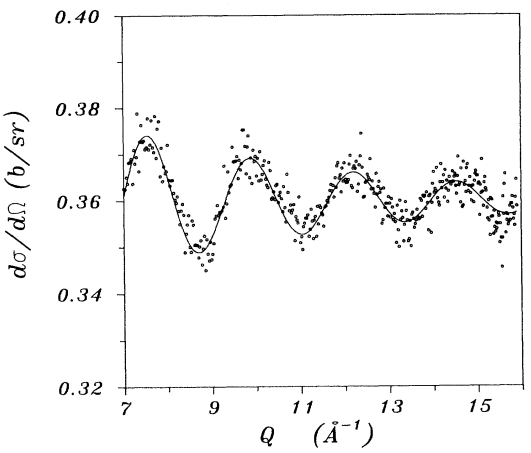

FIG. 2. $d\sigma/d\Omega$ for liquid I_2: experimental data (dots) and fit according to Eq. (5) (solid line).

have derived the intermolecular structure factor $D_M(Q)$ as

$$D_M(Q)=\frac{1}{4b_I^2}\left[\frac{d\sigma}{d\Omega}-\left[\frac{d\sigma}{d\Omega}\right]_{\text{gas}}\right], \tag{6}$$

where b_I is the scattering length of the iodine atom and $(d\sigma/d\Omega)_{\text{gas}}$ was calculated, following Ref. [13], with $d=2.70$ Å and with a I-I stretching frequency $E_{\text{vib}}=26.62$ meV [14]. $d\sigma/d\Omega$, $(d\sigma/d\Omega)_{\text{gas}}$, and $D_M(Q)$ functions are plotted in Fig. 3. As far as the $D_M(Q)$ function is concerned, we note a well-defined structure in the first peak and an intense second peak. Moreover no oscillations are visible beyond ~ 7 Å^{-1}. Therefore the intermolecular structure factor is the appropriate function to be Fourier transformed in r space, in order to reduce truncation errors in the intermolecular atom-atom pair correlation function, $g(r)$. This yields

$$g(r)=1+\frac{1}{2\pi^2\rho_M}\int_0^{Q_M} D_M(Q)M(Q)\frac{\sin Qr}{Qr}Q^2dQ\ , \tag{7}$$

where ρ_M is the molecular number density and $M(Q)$ is an apodization function, defined as

$$M(Q)=\begin{cases}1 & \text{if } 0\le Q\le Qi\\ \frac{1}{2}\left[1+\cos\frac{\pi(Q-Q_i)}{(Q_M-Q_i)}\right] & \text{if } Q_i\le Q\le Q_M\end{cases} \tag{8}$$

with $Q_i=8$ Å^{-1} and $Q_M=15.9$ Å^{-1}. The use of the smooth function $M(Q)$ is to avoid the sharp cutoff occurring at $Q=Q_M$, which would produce unphysical ripples in r space with periodicity $2\pi/Q_M$. In Table II we report the $d\sigma/d\Omega$ and $D_M(Q)$ and in Table III the $g(r)$ function, the latter is also shown in Fig. 4(a). In this figure the minimum approaching distance of two iodine atoms not belonging to the same molecule occurs at $r\sim 2.8$ Å. This implies that describing the I-I interaction by a Lennard-Jones effective term, the σ value might be settled equal to about 3.0 Å.

The main peaks of the $g(r)$ function are centered around $r=4.2$ and 6.1 Å, respectively. The ratio of these positions is much lower than the value found in oxygen and nitrogen, where no orientational correlations are detectable, while it agrees with those found in Cl_2 and Br_2. However since these main peaks are asymmetric, they cannot be simply ascribed to the first and second neighboring shells. Indeed from the $n(r)=4\pi r^2\rho_S g(r)$ function four subshells can be identified in the range $3\le r\le 7$ Å. In Fig. 4(b) the $n(r)$ function is shown together with its decomposition into four symmetric shapes ($S1$,$S2$,$S3$,$S4$): the first subshell ($S1$) has been obtained by symmetrizing the $n(r)$ function up to its first maximum. $S1$ shape has then been subtracted from $n(r)$ and this procedure has been iterated to produce the final decomposition. The peak positions r and the coordination numbers for each subshell n are reported in Table IV. We note that in this procedure the choice of meaningful peak positions for each subshell can be made in a r range which corresponds to an uncertainty in n values of $\le 10\%$.

As far as the comparison with the data of Refs. [1] and [2] is concerned (see Fig. 5), we note some discrepancies

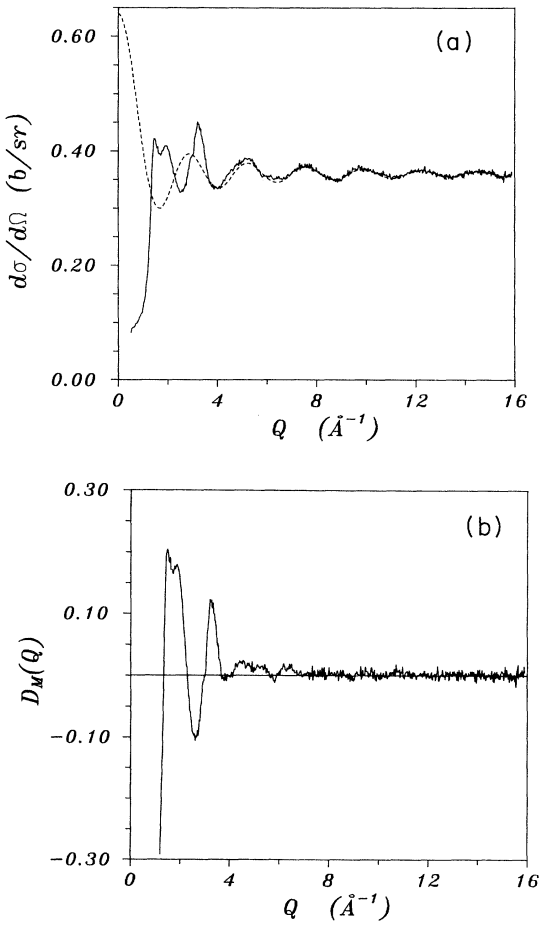

FIG. 3. (a) Atomic differential cross section: experimental $d\sigma/d\Omega$ (solid line); $(d\sigma/d\Omega)_{\text{gas}}$ according to Ref. [12] (dashed line). (b) $D_M(Q)$ function.

TABLE II. Differential scattering cross section and intermolecular structure factor for saturated liquid I_2 at $T=409$ K.

Q (Å^{-1})	$d\sigma/d\Omega$	$D_M(Q)$	Q (Å^{-1})	$d\sigma/d\Omega$	$D_M(Q)$
0.1040	0.0311	−0.8950	5.4335	0.3824	0.0126
0.1977	0.0321	−0.8870	5.5224	0.3754	0.0051
0.2911	0.0415	−0.8830	5.6111	0.3683	−0.0016
0.3844	0.0407	−0.8700	5.6997	0.3668	0.0027
0.4778	0.0738	−0.8300	5.7881	0.3565	−0.0084
0.5712	0.0906	−0.8068	5.8764	0.3559	−0.0025
0.6645	0.0925	−0.7512	5.9645	0.3559	0.0040
0.7578	0.0993	−0.6845	6.0524	0.3561	0.0102
0.8511	0.1086	−0.6132	6.1402	0.3567	0.0160
0.9444	0.1159	−0.5470	6.2278	0.3518	0.0105
1.0377	0.1345	−0.4638	6.3152	0.3520	0.0127
1.1309	0.1642	−0.3655	6.4025	0.3554	0.0191
1.2241	0.2139	−0.2375	6.4896	0.3560	0.0191
1.3172	0.3022	−0.0471	6.5765	0.3523	0.0099
1.4104	0.4005	0.1536	6.6632	0.3520	0.0057
1.5034	0.4197	0.2048	6.7497	0.3522	0.0015
1.5965	0.4074	0.1916	6.8361	0.3586	0.0076
1.6895	0.3949	0.1708	6.9223	0.3561	−0.0025
1.7824	0.4013	0.1772	7.0083	0.3626	0.0035
1.8753	0.4088	0.1801	7.0940	0.3636	0.0000
1.9682	0.4085	0.1645	7.1796	0.3690	0.0048
2.0610	0.3970	0.1256	7.2650	0.3679	−0.0013
2.1537	0.3792	0.0735	7.3502	0.3663	−0.0074
2.2464	0.3594	0.0171	7.4352	0.3726	0.0018
2.3390	0.3442	−0.0303	7.5200	0.3714	−0.0012
2.4316	0.3344	−0.0664	7.6046	0.3720	0.0001
2.5241	0.3282	−0.0934	7.7732	0.3755	0.0100
2.6165	0.3282	−0.1058	7.8571	0.3714	0.0059
2.7089	0.3425	−0.0889	7.9408	0.3658	−0.0003
2.8011	0.3533	−0.0742	8.0244	0.3643	0.0015
2.8933	0.3821	−0.0231	8.1077	0.3644	0.0060
2.9854	0.3925	−0.0012	8.1907	0.3594	0.0018
3.0775	0.4194	0.0536	8.3562	0.3569	0.0053
3.1694	0.4398	0.0995	8.4386	0.3548	0.0049
3.2613	0.4460	0.1220	8.5208	0.3489	−0.0032
3.3531	0.4264	0.0995	8.6027	0.3504	0.0011
3.4448	0.4089	0.0812	8.6844	0.3476	−0.0031
3.5364	0.3849	0.0511	8.8471	0.3449	−0.0091
3.6278	0.3593	0.0169	8.9281	0.3470	−0.0072
3.7192	0.3434	−0.0015	9.0088	0.3484	−0.0071
3.8105	0.3418	0.0035	9.1428	0.3568	0.0025
3.9017	0.3378	0.0019	9.2229	0.3578	0.0009
3.9928	0.3344	−0.0016	9.3027	0.3561	−0.0059
4.0838	0.3385	0.0059	9.3823	0.3616	0.0004
4.1746	0.3424	0.0102	9.5406	0.3685	0.0062
4.2654	0.3489	0.0171	9.5194	0.3687	0.0040
4.3560	0.3548	0.0209	9.6979	0.3752	0.0138
4.4465	0.3587	0.0196	9.8541	0.3649	−0.0064
4.5369	0.3665	0.0244	9.9319	0.3708	0.0044
4.6272	0.3642	0.0109	10.0090	0.3652	−0.0050
4.7173	0.3745	0.0202	10.1890	0.3685	0.0052
4.8073	0.3758	0.0141	10.2910	0.3681	0.0080
4.8972	0.3846	0.0225	10.3920	0.3618	0.0005
4.9869	0.3827	0.0135	10.4930	0.3595	0.0004
5.0765	0.3853	0.0140	10.9900	0.3508	−0.0024
5.1660	0.3871	0.0153	11.4740	0.3572	0.0012
5.2553	0.3872	0.0155	12.0360	0.3637	−0.0032
5.3445	0.3825	0.0091	12.4880	0.3640	−0.0006

TABLE III. Atom-atom intermolecular pair correlation function for saturated liquid I_2 at $T=409$ K.

r (Å)	$g(r)$
3	0.119
3.2	0.207
3.4	0.431
3.6	0.702
3.8	0.993
4	1.379
4.2	1.584
4.4	1.45
4.6	1.304
4.8	1.191
5	1.007
5.2	0.899
5.4	0.915
5.6	0.894
5.8	0.949
6	1.117
6.2	1.138
6.4	1.08
6.6	1.015
6.8	0.949
7	0.918
7.5	0.943
8	0.981
8.5	1.008
9	0.993
9.5	1.026
10	1.038
10.5	1.013
11	0.977
12	0.992
13	0.994
14	1.016
15	0.999
16	1
17	0.995
17.1	0.995
18	1.008
19	0.998
20	1.003

in the first peak between our results and the earlier neutron data. In the latter case a poorer collimation of the neutron beam might have caused problems in the background subtraction in the low 2θ range.

In the case of x-ray data a marked disagreement with our data extends over the whole Q range: similar discrepancies have already been evidentiated in the other halogens [3].

TABLE IV. Average distance and number of first neighboring atoms n, corresponding to the four subshells in Fig. 4(b).

r (Å)	n (atoms)
4.3	7.6
4.9	1.8
5.5	3.8
6.2	7.5

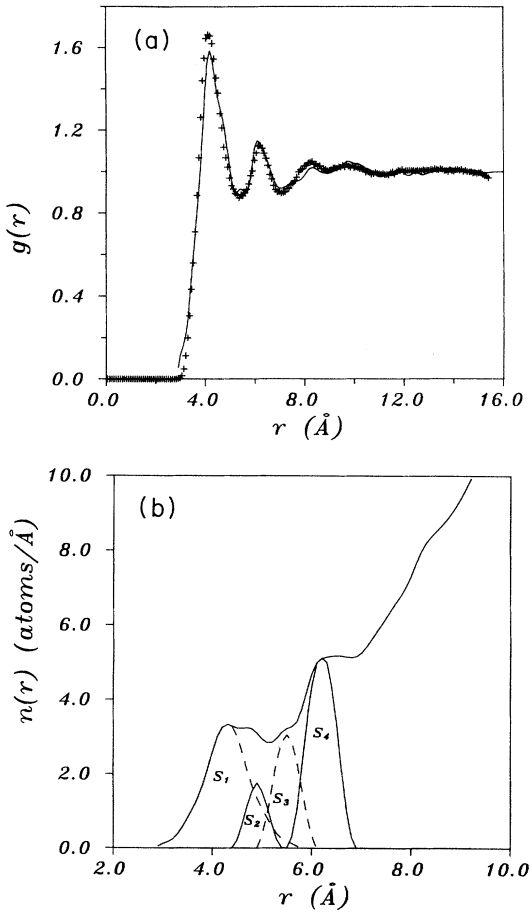

FIG. 4. (a) Intermolecular atom-atom pair correlation function: experimental data (solid line); simulation from Ref. [5] (crosses). (b) $n(r)$ function and its decomposition into the first four subshells.

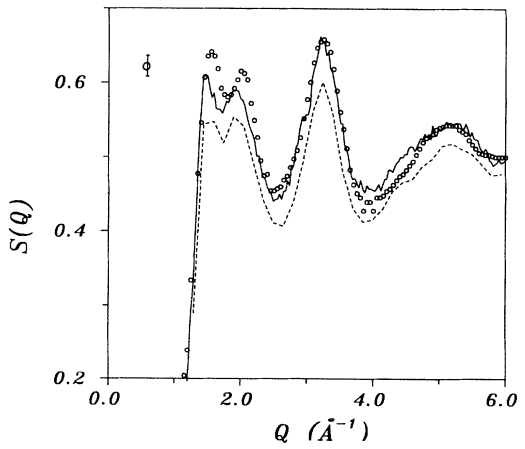

FIG. 5. $S(Q)$'s functions: present data (solid line); neutron data of Ref. [1] (open circles); (dashed line) x-ray data from Ref. [2]. ϕ represents the estimated mean uncertainty for the data of Ref. [1]; for the present data the uncertainty is $\pm 6\times 10^{-3}$ (which is almost the thickness of the line) and is mainly due to the statistical accuracy.

DISCUSSION

In order to investigate the presence of the orientational correlations in the structure of liquid iodine, the Egelstaff, Page, and Powles criterion [15] has been followed. This states, for a diatomic molecule with completely uncorrelated orientations, that

$$D_M(Q)=f_{2u}(Q)[S_C(Q)-1] \tag{9}$$

with

$$f_{2u}(Q)=\left[\frac{\sin(Qd/2)}{Qd/2}\right]^2, \tag{10}$$

where $S_C(Q)$ is the structure factor for molecular centers.

From Eq. (9) it follows that

$$S_C(Q)=1+\frac{D_M(Q)}{f_{2u}(Q)} . \tag{11}$$

A regular behavior of the $S_C(Q)$ function is an indication of the reliability of the uncorrelated model. This is achieved either if $D_M(Q)$ and $f_{2u}(Q)$ have similar zeros, that is at $Q=2n\pi/d$, or if both functions behave such that $S_C(Q)$ remains finite and positive. From Fig. 6 it appears that there are strong irregularities in the $S_C(Q)$ function already at the first peak position. The same test performed on liquid chlorine [16], at the same T/T_C value [17], gave a regular $S_C(Q)$ pattern up to Q values ($\sim$2.5 Å) beyond the first peak. This indicates that the orientational correlations present in liquid iodine are even stronger than those found in chlorine.

In order to investigate the contribution of these correlations to the intensity distribution in the $D_M(Q)$ function, the latter can be compared with a model function $D_u(Q)$ for an uncorrelated liquid. The model function can be obtained inserting into Eq. (9) a $S_C(Q)$ function derived for an "equivalent monoatomic" liquid [3]. As an equivalent monoatomic liquid we choose an ensemble of atoms interacting via the Lennard-Jones potential with parameters $\sigma=4.33$ Å and $\varepsilon/k_B=655$ K [18]. The $D_u(Q)$ function (Fig. 7) shows a first intense and slightly asymmetric peak around $Q\leq 2$ AÅ^{-1}, a very weak second peak at $Q\sim 3.5$ Å^{-1}, and no intensity beyond $Q\sim 4$ Å^{-1}. Furthermore below 4 Å^{-1} the $D_M(Q)$ function shows very large discrepancies with the $D_u(Q)$ model; that is a clearly double structured first peak, twice as intense as in $D_u(Q)$, a deep minimum and a second peak of the same order of magnitude of the first one.

These discrepancies are larger than those found in the case of liquid chlorine, thus pointing out that the effects of the potential anisotropy are strongly enhanced in the structure of liquid iodine. This is also confirmed by the behavior of the $n(r)$ function. Indeed while in the case of liquid chlorine only two first-neighbors subshells have been identified in the range $3\leq r\leq 6$ Å, in liquid iodine there are four of these in the same r region, with an average FWHM $\sim$1.2 Å in Cl_2 and $\sim$0.7 Å in I_2. This suggests a better definition of the relative orientations of neighboring molecules in iodine. We notice that the center-of-mass position of the first ($S1$ and $S2$) and second ($S3$ and $S4$) couple of subshells are in the same ratio as for the two subshells identified in the case of chlorine. This suggests that in liquid iodine well-defined orientations are present, while in liquid chlorine the molecules can continuously experience the different orientations.

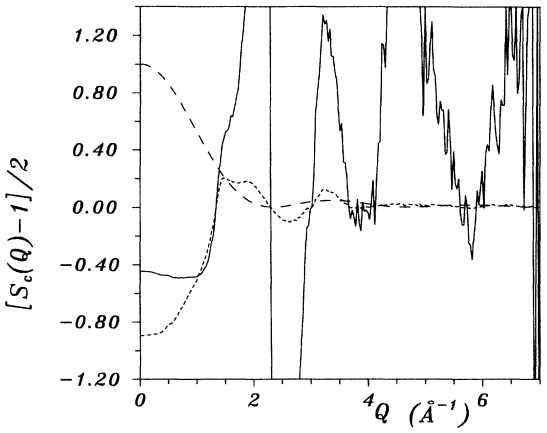

FIG. 6. $[S_C(Q)-1]/2$ for liquid iodine (solid line); for comparison we also report $f_{2u}(Q)$ (long-dashed line) and $D_M(Q)$ (short-dashed line).

Finally we compare the experimental pair correlation function with that derived by computer simulation using the potential model $A2$ [5]. This comparison is reliable and conclusive, due to both the high accuracy of our data and the wide Q range explored. In this context we want to stress that any comparison between simulation and experimental data is better performed in r space in that it avoids the truncation errors arising from the finite dimensions of the simulation box.

From Fig. 4(a) it results that the $A2$ potential model describes very successfully the microscopic structure of the liquid iodine as revealed through the $g(r)$ function.

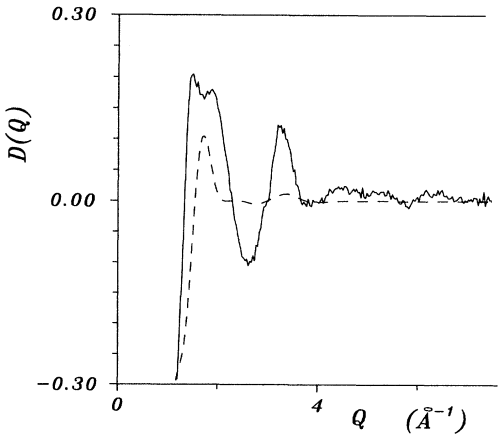

FIG. 7. Experimental $D_M(Q)$ (solid line); $D_u(Q)$ (dashed line).

CONCLUSIONS

From the present measurements we conclude that strong and well-defined orientational correlations exist in liquid iodine. Moreover the $A2$ potential reproduces very well the experimental radial distribution function. As a consequence liquid iodine is probably the best example, among diatomic fluids, in order to study the influence of the potential anisotropy in determing the orientational correlations.

Therefore at this stage a complete study of the whole orientational configurations in this liquid by a computer simulation experiment, using the $A2$ potential model, is to be attempted. However it is to be noted that this potential model gives a poorer agreement in liquid bromine and chlorine. In the latter case indeed a density-dependent scaling factor on the intermolecular distance in the simulated $g(r)$ function is to be invoked [16,19].

Another point which deserves to be clarified concern the discrepancies between the $S(Q)$ functions derived from neutron and x-ray experiments. Indeed these have not seemed to decrease by increasing the atomic number, going from chlorine to iodine. This evidence suggests that the failure of the isolated atom approximation for the x-ray form factor is not completely ascribable to the bonding electron clouds. Finally the implications of such strong correlations on the microscopic dynamics of iodine ought to be investigated.

ACKNOWLEDGMENTS

This work has been partially supported by GNSM of CNR and INFM. We gratefully acknowledge the technical assistance of Mr. J. P. Ambroise (Laboratoire Leon Brillouin, CEN, Saclay).

*Author to whom all correspondence should be addressed.

[1] P. Bosi, F. Cilloco, and M. A. Ricci, Mol. Phys. **40**, 1285 (1980).
[2] C. Van der Marel, W. Bras, and W. Van der Lugt, Mol. Phys. **64**, 445 (1988).
[3] C. Andreani, J. C. Dore, and F. P. Ricci, Rep. Prog. Phys. **54**, 731 (1991).
[4] P. M. Rodger, A. Stone, and D. J. Tildesley, Chem. Phys. Lett. **145**, 365 (1988).
[5] P. M. Rodger, A. Stone, and D. J. Tildesley, Mol. Phys. **63**, 173 (1988).
[6] I. L. Karle, J. Chem. Phys. **23**, 1739 (1955).
[7] F. Van Bolhuis, P. B. Koster, and T. Migchelsen, Acta Crystallogr. **23**, 90 (1967).
[8] K. Takemura, S. Minomura, O. Shimomura, and Y. Fujii, Phys. Rev. Lett. **45**, 1881 (1980).
[9] Y. Fujii, K. Hase, N. Hamaya, Y. Ohishi, A. Onodera, O. Shimomura, and K. Takemura, Phys. Rev. Lett. **58**, 796 (1987).
[10] J. P. Ambroise, M. C. Bellissent-Funel, and R. Bellissent, Rev. Phys. Appl. **19**, 731 (1984); J. P. Ambroise and R. Bellissent, ILL Workshop on Position Sensitive Detectors, edited by E. Convert and B. J. Forsyth (Academic, London, 1983).
[11] C. Petrillo and F. Sacchetti, Acta Crystallogr. Sect. A **46**, 440 (1990).
[12] S. W. Lovesey, Theory of Neutron Scattering from Condensed Matter (Clarendon, Oxford, 1984), Vol. 1, Table 1.1.
[13] P. A. Egelstaff, and A. K. Soper, Mol. Phys. **40**, 569 (1980).
[14] D. H. Rank and B. S. Rao, J. Mol. Spectrosc. **13**, 34 (1964).
[15] P. A. Egelstaff, D. T. Page, and J. G. Powles, Mol. Phys. **20**, 881 (1971).
[16] M. C. Bellissent-Funel, U. Buontempo, C. Petrillo, and F. P. Ricci, Mol. Phys. **71**, 253 (1990).
[17] The subscrpt c in this case indicates the critical-point value.
[18] The Lennard-Jones parameters have been estimated, in the framework of the corresponding-states principle, from the critical parameters of liquid iodine (see Ref. [3]).
[19] M. C. Bellissent-Funel, U. Buontempo, C. Petrillo, and F. P. Ricci, Mol. Phys. (to be published).